

Metal-wire terahertz time-domain spectroscopy

Markus Walther,^{a)} Mark R. Freeman, and Frank A. Hegmann^{b)}
Department of Physics, University of Alberta, Edmonton, Alberta T6G 2J1, Canada

(Received 15 June 2005; accepted 1 November 2005; published online 21 December 2005)

Terahertz (THz) pulses propagating on a metal-wire waveguide are used to perform terahertz time-domain spectroscopy of lactose powder dispersed on top of the wire. The THz pulses are generated by a photoconductive switch at one end of the metal wire and are detected at the other end by electro-optic sampling in a ZnTe crystal that can be moved parallel to the axis of the metal wire. A large enhancement in the peak amplitude of the THz signal is observed by contacting the metal wire to one of the electrodes of the photoconductive switch. The propagation characteristics of the THz pulse along the metal wire and near its end are studied. Potential applications of metal-wire terahertz time-domain spectroscopy are discussed. © 2005 American Institute of Physics.
 [DOI: 10.1063/1.2158025]

Terahertz time-domain spectroscopy (THz-TDS) has developed into a versatile tool in the far-infrared spectral region. In such experiments, free-space-coupled subpicosecond terahertz (THz) pulses are analyzed after propagating through a sample allowing the complex dielectric constants to be extracted. Collimation and subsequent focusing of the THz radiation by suitable far-infrared optics allows significant reduction in the investigated sample volumes. However, due to diffraction limitations, the THz focal spot size and, hence, the required sample dimensions are still comparably large. Therefore millimeter-sized samples are still required with at least a few milligrams of material as is the case for many molecular samples.^{1,2} Spectroscopy with wave-guided THz pulses is one possibility that may help overcome such limitations. Integrated waveguide structures such as coplanar transmission lines³ or waveguide resonators⁴ have enabled the investigation of much smaller sample sizes since only the area in close proximity to the micron-sized waveguide has to be covered. Also, recent progress in efficiently transmitting subpicosecond THz pulses along nonintegrated (open) waveguide structures⁵⁻⁹ has triggered novel applications that make it possible to measure, for example, the dielectric constants of extremely thin layers of materials.¹⁰ All these approaches, however, generally suffer from considerable loss and dispersion of the guided THz pulses, severely limiting the propagation path lengths and therefore the active interaction region, which would inhibit the investigation of weakly absorbing materials. Very recently, however, single metal wires have been demonstrated that guide radially polarized THz pulses over long distances showing low loss and very low group velocity dispersion.¹¹⁻¹⁴ In this letter, we demonstrate spectroscopy using THz pulses guided along such a metal wire. A simple photoconductive emitter in contact with the wire tip is used to effectively launch subpicosecond THz pulses into a metal wire which are electro-optically detected^{15,16} after propagating and interacting with a sample substance deposited on the wire. Our approach explicitly does not require far-infrared optics or complex THz pulse coupling schemes, resulting in a very compact, simple, and robust setup.

We used an 11-cm-long platinum/iridium wire with a diameter of 254 μm and with a sharp tip on one side and a

flat end on the other. The tip was in contact with the positive electrode of a photoconductive (PC) THz emitter, as shown in Fig. 1(a). The relatively simple layout of the PC emitter consists of two coplanar 100- μm -wide striplines separated by an 80 μm gap deposited on a semi-insulating-GaAs substrate. Two 2-mm-thick polystyrene disks are used (not shown in Fig. 1) to rigidly mount the wire in the setup. The wire tip contacted the anode close to the edge of a tilted 1-mm-wide emitter chip, as shown in Fig. 1(b). The output of a mode-locked Ti:sapphire laser (50 fs, 800 nm, 75 MHz repetition rate) is split into an excitation beam and a detection beam. The excitation pulses, with an average power of 55 mW, are focused between the two coplanar strip lines of the emitter close to the anode and close to the metal tip. The detection beam propagates collinearly with the guided THz pulses at a distance of about 1 mm from the surface of the metal wire and illuminates a spot on a 1-mm-thick (110)-ZnTe crystal which has been orientated to electro-optically detect the z component of the radially polarized electric field of the guided THz pulse using a pair of balanced photodiodes.^{15,16} The detector beam path can be scanned with a variable delay for sampling the THz pulse wave form and the detection crystal can be translated in the x direction in order to probe the THz wave forms at different positions along the wire axis. Note that we detected no THz signal without the metal-wire waveguide, as would be expected since the angle between the metal wire axis and the line

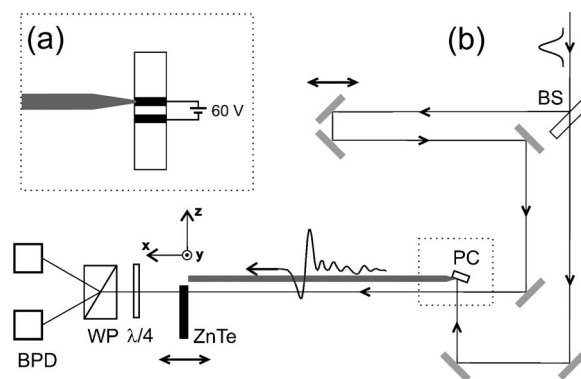


FIG. 1. (a) Side view of the photoconductive emitter with the wire tip contacting the positive electrode. (b) The experimental setup. (BS=beam splitter, PC=photoconductive switch emitter, WP=Wollaston polarizer, BPD=balanced photodiodes.)

^{a)}Electronic mail: mwalther@phys.ualberta.ca

^{b)}Electronic mail: hegmann@phys.ualberta.ca

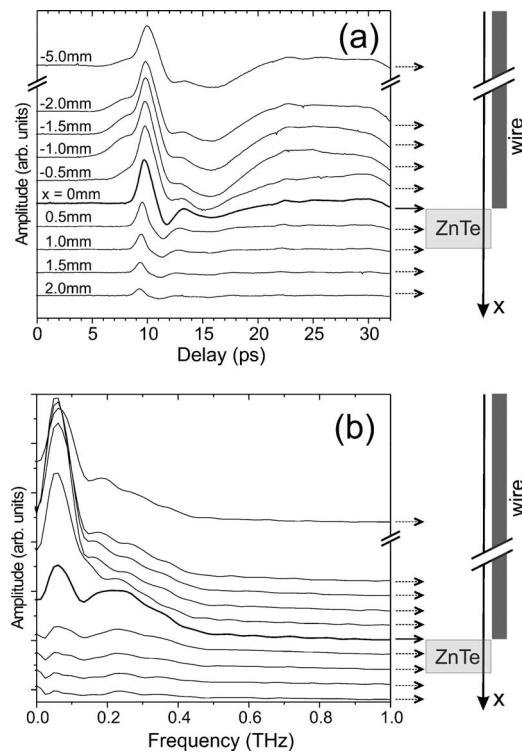


FIG. 2. (a) THz pulses measured at different positions along the metal wire axis. (b) Corresponding frequency spectra of the THz pulses in (a). The collimation of the 800 nm sampling beam, which travels alongside the THz pulse parallel to the wire, was optimized for the $x=0$ position. This may account for slight distortions in the THz wave form at positions <0 in (a).

normal to the emitter surface (main emission direction) was $\sim 80^\circ$, as depicted in Fig. 1(b).

Figure 2(a) shows the THz pulse wave forms measured with the ZnTe detection crystal at different positions along the metal-wire axis. The value for $x=0$ corresponds to the case where the front surface of the crystal is lined up with the flat end of the wire, as indicated in the schematics in Fig. 2. The peak of the THz pulses does not shift in time, indicating pulse propagation at the free-space velocity of light as reported previously for a metal wire THz pulse waveguide.^{11,14} As a consequence of the very low loss and low group velocity dispersion, the THz wave forms essentially do not change as they propagate along the metal wire. At around $x=0$, however, the wave form dramatically changes shape, and for $x > 0$, where the THz pulse is no longer guided, the THz pulse progressively diminishes with increasing distance from the wire end. The corresponding frequency spectra, as seen in Fig. 2(b), show that the THz pulses essentially consist of two broad spectral components: one centered at around 80 GHz and a band with a maximum at around 240 GHz. Very similar THz spectra consisting of two such components have been observed previously for THz pulses coupled to metal-wire waveguides from a radial photoconductive antenna.¹² Whereas the low-frequency component dominates the THz signal along the wire, the contribution at higher frequencies becomes comparable in intensity at the end of the wire. Interestingly, we find that we achieve the largest spectral bandwidth at exactly $x=0$, i.e., when the front surface of the ZnTe crystal is lined up with the flat end of the wire. Consequently, we chose this detector position as the point of operation throughout the rest of this letter. We photoexcited the emitter at the position where the wire contacted the electrode [see

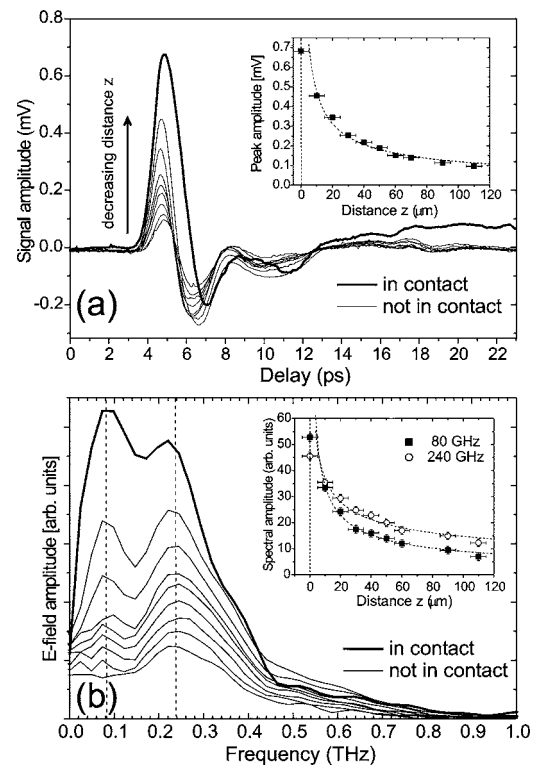


FIG. 3. (a) THz pulses measured with the THz emitter at different distances from the tip of the metal wire ($10 \mu\text{m}$ steps). The inset shows the peak amplitude of the pulses versus the distance z . The dashed line is a best fit to the data showing $z^{-0.6}$ behavior. (b) Corresponding frequency spectra. The inset shows the amplitude of the spectral components at 80 and 240 GHz as a function of the distance z away from the emitter. The dashed lines are best fits showing $z^{-0.6}$ and $z^{-0.4}$ dependence, respectively.

Fig. 1(a)]. If this was not done, then the generated THz pulses had to propagate a short distance along the coplanar electrodes before they would couple into the wire. This resulted in considerable pulse broadening due to group velocity dispersion along the coplanar striplines similar to recent observations for the coupling of THz pulses to a metal-tip antenna.¹⁷ In principle, the metal-wire tip could be contacted to the emitter at any position on the electrode of the emitter. However, we found that contacting the metal wire close to the edge of the emitter, as shown in Fig. 1(a), gave optimized coupling and minimized artifacts in the THz wave forms due to reflections at the end of the striplines. In order to establish contact between the metal wire and the electrode, the THz emitter was mounted on a translation stage so that it could be moved in the z direction [see Fig. 1(b)] towards the tip of the metal wire. Figure 3(a) shows the THz pulse wave forms as a function of the separation distance in the z direction between the photoconductive switch emitter and the tip of the metal wire ($10 \mu\text{m}$ step size), where $z=0$ is the contacted position. As the emitter approaches the wire, the generated THz field couples more strongly to the wire resulting in larger THz signals. The signal amplitude varies as $1/z^{0.6}$, as determined from a best fit and shown by the dashed line in the inset of Fig. 3(a), as long as the emitter and wire are not in contact. We want to point out that in contrast to this behaviour, a $1/z$ dependence was observed for the radial decay of the peak electric field of the THz pulses at the end of the wire, in agreement with previous studies.^{12,14} As soon as the tip is in contact with the anode the THz wave form suddenly changes shape and the peak THz amplitude acquires its

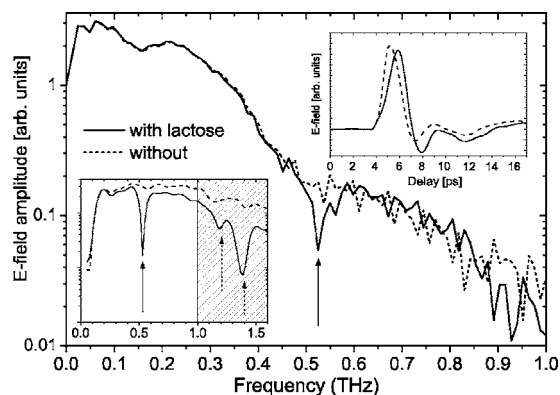


FIG. 4. Frequency spectra of THz pulses propagated along the wire with (solid line) and without lactose powder on the wire (dashed line). The upper inset shows the corresponding THz pulses. The arrow indicates a distinct absorption of lactose at 0.53 THz. The lower inset shows THz transmission spectra of lactose recorded with a conventional THz-TDS setup. The arrows indicate absorption bands of lactose.

maximum value. This characteristic change can be attributed to the contribution of a low frequency component to the signal. Figure 3(b) shows the frequency spectra of the wave forms in Fig. 3(a). As discussed earlier, there are two spectral components to the THz signal. These contributions, however, show a significantly different distance dependence. Whereas the band at higher frequencies dominates the spectra at larger distances, the low frequencies increasingly contribute at shorter separations as well as when contact is made. The inset shows the amplitudes of the two spectral components centered at 80 and 240 GHz together with best fits to the data showing $1/z^{0.6}$ and $1/z^{0.4}$ dependence, respectively (dashed lines). Further investigations, in particular with regard to the origin of the two spectral components, are currently being pursued and will be published elsewhere. Interestingly, we observe a dramatic signal increase at low frequencies but also a sudden drop at frequencies above 0.45 THz when contact is made. As a consequence it appears favorable for spectroscopic applications to work in contact mode for investigations in the low frequency region below ~ 0.45 THz whereas an operation at a short distance around $10 \mu\text{m}$ would be preferred for the observation of features in the range from 0.45–1.0 THz.

Using our metal-wire spectrometer in contact mode, we investigated the absorption of polycrystalline lactose powder (Becton-Dickinson Co.) dispersed on top of the wire. At room temperature lactose displays a number of sharp resonances in the far-infrared region originating from external and internal molecular vibrations which can be observed by standard free-space coupled THz-TDS.^{18,19} The lower inset in Fig. 4 shows a THz transmission spectrum through a 1-mm-thick pressed disk of lactose powder at room temperature recorded with a standard THz-TDS setup in a nitrogen purged environment. A reference spectrum taken without the sample in the beam path is also shown (dotted line). Distinct absorption features from the lactose sample are observed as indicated by the arrows. In particular a prominent absorption at 0.53 THz can be found in the region accessible by our metal-wire spectrometer (unshaded region). For the metal-wire THz-TDS measurement, 1 mg of lactose powder was dispersed over a 55-mm-long section of the wire between the THz emitter and the detector. The guided THz pulses with and without lactose on the wire are shown in the upper inset of Fig. 4. The corresponding frequency spectra in Fig. 4 of

the time-domain traces show the expected absorption feature at 0.53 THz, which is absent in the reference spectrum. In contrast to free-space THz-TDS, purging the metal-wire spectrometer with dry nitrogen was not required since water vapour absorption was not observed in the reference spectrum.

Metal-wire THz-TDS combines the advantages of waveguide spectroscopy for measuring small sample amounts in close proximity to the confined THz field with the capability to increase the interaction region by simply extending the propagation length along the wire. This potentially allows either the investigation of even weakly absorbing materials such as biomolecules or extremely thin films deposited on the metal wire. Note that strong waveguide dispersion has been observed for THz pulses propagating along a metal wire coated with thin dielectric films, even if the dielectric itself is nondispersive, leading to highly chirped signals.²⁰ Although this has implications on practical wire lengths for the spectroscopy of thin films it does not effect the power absorption in the material and therefore would still allow the observation of characteristic absorption features, as demonstrated here for lactose. With future improvements, the investigation of molecular monolayers deposited on a metal-wire terahertz time-domain spectrometer may become possible.

In conclusion, we report a novel and compact metal-wire THz time-domain spectrometer setup. Contacting a simple photoconductive emitter to a metal wire resulted in an enhanced coupling of THz pulses into the wire. A movable THz pulse detector allowed us to investigate the THz field as it propagated along the wire and radiated from the end of the wire. Molecular spectroscopy of lactose dispersed on top of the wire was demonstrated.

The authors acknowledge financial support from the Natural Sciences and Engineering Research Council of Canada (NSERC), iCORE, and the NSERC Nano Innovation Platform (NanoIP).

¹A. G. Markelz, A. Roitberg, and E. J. Heilweil, *Chem. Phys. Lett.* **320**, 42 (2000).

²M. Walther, B. Fischer, M. Schall, H. Helm, and P. Uhd Jepsen, *Chem. Phys. Lett.* **332**, 389 (2000).

³R. Sprik, I. N. Duling, C. C. Chi, and D. Grischkowsky, *Appl. Phys. Lett.* **51**, 548 (1987).

⁴M. Nagel, P. H. Bolivar, M. Brucherseifer, H. Kurz, A. Bosserhoff, and R. Buttner, *Appl. Opt.* **41**, 2074 (2002).

⁵T.-I. Jeon and D. Grischkowsky, *Appl. Phys. Lett.* **85**, 6092 (2004).

⁶G. Gallot, S. P. Jamison, R. W. McGowan, and D. Grischkowsky, *J. Opt. Soc. Am. B* **17**, 851 (2000).

⁷R. Mendis and D. Grischkowsky, *J. Appl. Phys.* **88**, 4449 (2000).

⁸R. W. McGowan, G. Gallot, and D. Grischkowsky, *Opt. Lett.* **24**, 1431 (1999).

⁹R. Mendis and D. Grischkowsky, *Opt. Lett.* **26**, 846 (2001).

¹⁰J. Q. Zhang and D. Grischkowsky, *Opt. Lett.* **29**, 1617 (2004).

¹¹K. L. Wang and D. M. Mittleman, *Nature (London)* **432**, 376 (2004).

¹²T.-I. Jeon, J. Zhang, and D. Grischkowsky, *Appl. Phys. Lett.* **86**, 161904 (2005).

¹³Q. Cao and J. Jahns, *Opt. Express* **13**, 511 (2005).

¹⁴K. Wang and D. M. Mittleman, *J. Opt. Soc. Am. B* **22**, 2001 (2005).

¹⁵C. Winnewisser, P. Uhd Jepsen, M. Schall, V. Schyja, and H. Helm, *Appl. Phys. Lett.* **70**, 3069 (1997).

¹⁶Q. Wu and X.-C. Zhang, *Appl. Phys. Lett.* **71**, 1285 (1997).

¹⁷M. Walther, G. S. Chambers, Z. Liu, M. R. Freeman, and F. A. Hegmann, *J. Opt. Soc. Am. B* **22**, 2357 (2005).

¹⁸B. M. Fischer, Ph.D. thesis, Albert-Ludwigs University Freiburg, Germany, 2005.

¹⁹P. F. Taday, *Philos. Trans. R. Soc. London, Ser. A* **362**, 351 (2004).

²⁰N. C. J. van der Valk and P. C. M. Planken, *Appl. Phys. Lett.* **87**, 071106 (2005).